

# An Efficient Threshold And Region-Based Approach: Brain MRI Segmentation Using Fuzzy C-Means Adaptive Convolutional Long/Short-Term Memory

**AKM B. Hossain<sup>1</sup>, Md. Sah Bin Hj. Salam<sup>2</sup>, Muhammad S. Alam<sup>3</sup>,  
Ahmad Fadhil Yusof<sup>4</sup>, AKM Bellal Hossain<sup>5</sup>**

<sup>1</sup>. *School of Computing, Faculty of Engineering, Universiti Teknologi Malaysia, 81310, Johor Baharu, Johor, Malaysia, k.m.a@graduate.utm.my*  
<https://orcid.org/0000-0003-3877-7037>

<sup>2</sup>. *School of Computing, Faculty of Engineering, Universiti Teknologi Malaysia, 81310, Johor Baharu, Johor, Malaysia, sah@utm.my*  
<https://orcid.org/0000-0002-9282-3906>

<sup>3</sup>. *School of Computing, Faculty of Engineering, Universiti Teknologi Malaysia, 81310, Johor Baharu, Johor, Malaysia, University of Bisha, College of Computing and Information Technology, Department of Artificial Intelligence Sabt-al-Alaya, Saudi Arabia*  
*shamsul20@graduate.utm.my, alam@ub.edu.sa*  
<https://orcid.org/0000-0002-9419-3928>

<sup>4</sup>. *Faculty of Computing, Senior Lecturer, Universiti Teknologi Malaysia, 81310, Johor Baharu, Johor, Malaysia,*  
*ahmadfadhil@utm.my,*  
<https://orcid.org/0000-0002-1958-6318>

<sup>5</sup>. *College of Computing and Information Technology, Department of Information Systems, University of Bisha, Al-Namas 61977, Saudi Arabia*  
*bhosayn@ub.edu.sa*

All body organs, especially the most important ones, are controlled by the brain, as well as any dysfunction of these cells would immediately jeopardize the life of a person by causing other organs to collapse. The brain is regarded as the most important organ in a person's body as a result. A tumor is a disorder of the brain's cells that manifests as inflamed brain tissue. The likelihood of quickly curing sickness will increase with the early identification of such tumorous cells. The detection of brain tumors is now done using magnetic resonance imaging (MRI). Several approaches have been created for MRI segmentation and tumor detection in the newly emerging study subject of image processing and segmentation of MRI images. An efficient threshold and region-based segmentation technique termed fuzzy c-means adaptive convolutional long/short-

term memory (FCM-CLSTM) is proposed in this study, along with various morphological operations. To improve the MRI image quality, the following methods are first applied: normalized median filter (NMF), Histogram Equalization (HE), Contrast Limited Adaptive Histogram Equalization (CLAHE), and Brightness Preserving Dynamic Fuzzy Histogram Equalization (BPDFHE). The pixels are then divided into distinct classes using our suggested FCM-CLSTM approach's threshold and region-based segmentation, classification, and morphological operators, which are then used to find the tumor portion of the image with the highest intensity. The analysis is done on accuracy (88.24%), precision (87.66%), recall (87.66%), F1-score (87.66%), RMSE (0.3430), AMBE (0.0) and MSE (0.1176) with the existing methodologies. The findings of the proposed method achieved significant scores compared to the existing method in brain MRI segmentation.

**Keywords- Brain tumor, MRI, segmentation, Threshold and region, Fuzzy c-means adaptive convolutional long/short-term memory (FCM-CLSTM), Normalized median filter (NMF)**

## 1. Introduction

An innovative technical application for the analysis and interpretation of neuroimaging data is the segmentation of brain MRI data, Ajagbe et al. [1]. Artificial intelligence, computer science, neurology, and medical imaging are just a few of the topics covered in this interdisciplinary discipline. "Without the use of hazardous radiation, a non-invasive imaging technique called MRI creates three-dimensional, intricate anatomical images." Its exceptional soft tissue contrast, great spatial resolution, and capacity to distinguish between white matter, grey matter, and cerebrospinal fluid make it particularly valuable for brain imaging. However, medical practitioners may find it challenging to make sense of the massive quantity of data that MRI scans yield, Dash et al. [2]. This is when it becomes clear how important brain MRI segmentation is.

An MRI image can be divided into many segments, each of which represents a distinct anatomical feature or area of interest, using a technique known as brain MRI segmentation. This approach may be very helpful in the diagnosis, treatment planning, and disease monitoring of structures such as tumors, lesions, or anatomical changes via their detection, quantification, and visualization. MRI images were manually segmented by experts, a laborious process that included both intra- and inter-observer variation, Wadhwa et al. [3]. The development of artificial intelligence and machine learning has led to the development of automated and semi-automatic MRI segmentation techniques. These advanced algorithms learn from a vast number of annotated instances and adapt them to new scenarios, allowing them to rapidly segment data and reduce the possibility of human mistakes. Brain MRI segmentation poses a number of challenges. A number of factors, such as individual variances in brain architecture, changes in MRI collection techniques and scanner features, the presence of noise and artifacts, and a lack of high-quality, annotated training data, may have an impact on the segmentation algorithms' performance, Lillington et al. [4].

Furthermore, the interpretability of machine learning models in clinical contexts remains a challenge, sometimes referred to as the "black box problem." Despite these difficulties, research is still being done to improve the accuracy, consistency, and generalizability of brain MRI segmentation techniques. The segmentation of the brain using MRI is a critical step in

the processing of complicated neuroimaging data, Niu et al. [5]. MRI segmentation is finding new uses, such as advancing our knowledge of the structure and operation of the brain and helping with the diagnosis and management of neurological disorders. The use of state-of-the-art machine learning techniques has greatly enhanced the process and opened the door to the possibility of quicker, more accurate, and more consistent results. Although there are challenges, the potential for development is great, providing the development and improvement of brain MRI segmentation methods.

This research presents the Fuzzy C-Means Adaptive Convolutional Long/Short-Term Memory (FCM-CLSTM) approach as an approach for brain MRI segmentation. The remainder of the paper is divided into subsequent parts. The literature review, which is covered in Section 2, looks at the relevant works. A thorough explanation of the recommended technique is described in Section 3. Section 4 provides an evaluation of the results, and Section 5 concludes the study.

## **2. Related works**

Authors Dalca et al. [6] suggested an innovative method that "combined deep learning with traditional probabilistic atlas-based segmentation," reducing the requirement for manual segmentation in the development of a segmentation model for novel MRI scans. They conducted investigations with thousands of MRI scans of the brain, demonstrating that the suggested technique produced high accuracy for brain MRI segmentation work across a variety of MRI contrasts in a very short amount of time (about 15 seconds at test time on a GPU). A unique ensemble technique using several CNNs processing overlapping brain regions was demonstrated by authors of, Coupé et al. [7]. They suggested "AssemblyNet, two U-Net assemblies inspired by constitutional decision-making ."Such a parliamentary system might handle challenging decisions, unexpected challenges, and agreements. Their scan-rescan consistency and disease robustness were examined. AssemblyNet remained reliable in those situations. Two brain MRI programmed segmentation methods, FreeSurfer (FS) and Statistical Parametric Mapping (SPM) were tested by the researchers Palumbo et al. [8] for intra- and inter-method reproducibility. They examined intra- and inter-method reproducibility using "Pearson's correlation (r), Bland-Altman plot, and Dice index ."SPM consistently had higher GM and smaller WM and subcortical volumes than FS. When comparing the size of the brains of men and women, the OASIS dataset showed differences.

The researchers of Wu et al. [9] suggested the "deep convolutional neural network fusion support vector machine algorithm (DCNN-F-SVM)" method for segmenting brain tumors. It has three steps. They trained deep CNN to map image space to tumor marker space, used projected labels from CNN with an SVM classifier on test images, and trained a deep classifier by integrating CNN and SVM. Results on BraTS and self-made datasets demonstrated significantly better performance than individual CNN and integrated SVM methods. The researchers of, Anand et al. [10] provided a multimodal, medically aided, machine learning method for segmenting and classifying brain tumors. The "geometric mean filter" is applied as preprocessing to MRI images with noise. To better pinpoint key areas in a picture, fuzzy c-means algorithms do segmentation. "Grey-level co-occurrence matrix (GLCM)" is a

dimension-reduction and feature-extraction tool. The images were organized using a variety of ML methods. When compared to other algorithms for detecting and classifying brain tumors, the SVM RBF method performed best.

The authors of Vang et al. [11] demonstrated Synergy-Net, a network that utilized both global and local data perceives to segment MS lesions. The u-Net architecture was utilized for global segmentation, with Mask R-CNN supplementing it at the local level. The training results were better than those of simple ensembles when lower layers were shared amongst the branches, and analyzed two datasets including 765 and 21 novels. Researchers, Myint et al. [12] demonstrated an effective procedure for segmenting brain tumors by applying a threshold to extracted pixels, performing morphological procedures, and applying a Gaussian high pass filter. Combining thresholding and morphological extraction, they were able to isolate the tumor from its background. The RGB image was grayscaled and filtered to remove noise. The resultant picture has greater contrast, making tumor detection easier. This method assists doctors in finding brain tumors before surgery. The authors of Khairandish et al. [13] categorized brain MRI scans into benign and malignant tumors using an accessible data set and a CNN. Image categorization techniques based on deep learning (DL). Better accuracy of categorization was found using a CNN that employed several feature extraction techniques. In terms of classification, the suggested hybrid model used a combination of CNNs and an SVM, while in terms of detection, it used threshold-based segmentation. The authors of Arshad et al. [14] presented a two-pronged approach: (a) using “Multi-Scale Convolutional Neural Network (MSCNN)” architecture to create an efficient classification method for diagnosing brain tumors and (b) reducing the effect that “Rician noise has on the MSCNN’s performance”. The primary goal was to create a reliable model that would improve the accuracy and efficiency of current tumor detection methods. Consequently, the Bat technique with the “Fuzzy C-Ordered Means (BAFCOM) clustering technique” has been suggested by the authors of Alhassan et al. [15] for automatic segmentation in multimodal MRI images to diagnose brain tumors. The clustering algorithm of “BAFCOM, the Bat Algorithm, obtains the tumor by computing the distance between the tumor Region of Interest (RoI)” and the surrounding non-tumor RoI.

## **2.1. Problem statement**

In the context of the k-nearest neighbor (k-NN), Mittal et al. [20] algorithm's performance is influenced by the selection of k. MRI images of the dataset were severely affected by the noise. Self-Organizing Map (SOM), Mittal et al. [20] method that accepts the union of the trained network to a local optimum is possible. Some challenges with convolutional neural network (CNN), Muiz, Fayyaz et al. [17] utilization have surfaced as the area of medical image processing uses CNNs more and more. More computing expenses occur when the designs are designed to provide more effective outcomes and get deeper, and the quality of the input images rises. Due to its complexity and large number of parameters, AlexNet, Yazdan et al. [16] requires a lot of computing power and time to train. Overfitting can happen with AlexNet, particularly when training on smaller datasets. It can be challenging and expensive to get enough high-quality assigned MRI images for AlexNet training. The Adaptive Clip Limit Tile Size Histogram Equalization (ACLTSHE), Fawzi et al. [19] approach can have disadvantages

such as increased processing time, susceptibility to parameter adjustment, and possible computational complexity. Furthermore, it could not function as well in every situation or with every kind of image, which might sometimes result in less-than-ideal outcomes. To identify these challenges and overcome the problem with the help of the FCM-CLSTM method. The advantages of the proposed FCM-CLSTM method contain the one benefit of FCM is that, unlike hard segmentations, where the whole classification can change, if a pixel is contaminated by noise, the segmentation will only change fractionally. The following are some benefits of CLSTM networks that are capable of capturing long-term dependencies. For medical imaging applications, this integrated architecture has the potential to significantly increase the accuracy and reliability of brain tumor segmentation.

### 3. Methodology

In the initial stage of our research, we collected a dataset and employed the Normalized Median filter (NMF) as a preprocessing technique for the raw data. The technique of Histogram Equalization (HE) was employed to improve the image's contrast. The division process of an image into smaller blocks is achieved by the utilization of Contrast-Limited Adaptive Histogram Equalization (CLAHE). The BPDFHE approach has been offered as a technique for enhancing an image histogram. The Fuzzy C-Means Adaptive Convolutional Long/Short-Term Memory (FCM-CLSTM) method was proposed for image segmentation. Figure 1 displays the overall methodology of this study.

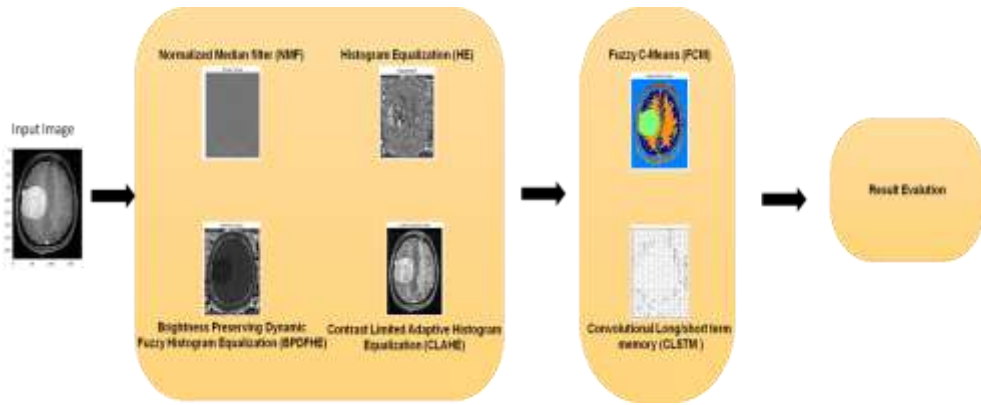


**Figure 1: Methodological Design**

#### 3.1 Data preprocessing

Preprocessing improves image quality and segmentation. Noise reduction, intensity leveling, skull stripping, spatial re-sampling, and data augmentation are included. These procedures make images consistent, artifact-free, and suitable for deep learning or classical segmentation algorithms to identify brain structures or regions of interest.

##### 3.1.1 Normalized Median Filter (NMF)

The median filter is a straightforward, non-linear, noise-reducing filter. In this, the desired noisy pixels are replaced with the median value of the nearby noisy pixels. The dimension of the analysis window determines the overall number of neighbors. The median value is often defined as the midway in a sorted series.

$$\text{Median } (X) = \text{Med } \{X_n\} \quad (1)$$

$$= X_n(Y + 1)/2, Y \text{ is Odd} \quad (2)$$

$$= 1/2[X_j(Y/2) + j(Y/2) + 1], Y \text{ is Even} \quad (3)$$

Aside from  $X_1, X_2$ , and  $X_3$ .  $XY$  refers to the set of adjacent pixels. The pixels in the image must all be arranged in a sequence that ascends or descends before the filter is applied. The pixel order for the sorted image will be  $X_{j1}, X_{j2}, X_{j3}, \dots$ , and  $X_{jY}$ , where  $Y$  is frequently odd. The filter replaces each pixel's value with the normalized median of its local neighborhood, which helps in removing salt-and-pepper noise while preserving image details.

### 3.1.2 Improve image contrast using Histogram Equalization (HE)

Assume a digital picture with  $[0, 1]^P$ , Probability range of grey levels. Distribution Equation (4) may be used to calculate the functions of the image:

$$Q(h_l) = \frac{m_l}{M} = 0, \dots, P-1 \quad (4)$$

Where  $m_l$  is the number of pixels in the picture with grey as level  $h_l$ , and  $h_l$  is the  $P^{\text{th}}$  grey level. Another method for computing the cumulative distribution function (CDF) is as follows:

$$B(h_l) = \sum_{j=0}^{j=l} Q(h_j) \quad (5)$$

$$l = 0, \dots, P-1, 0 \leq B(h_l) \leq 1 \quad (6)$$

Equation (5) is used by Histogram Equalisation (HE) to convert the input image's grey level  $T_l$  to grey level  $h_l$ . We, therefore have:

$$T_l = (P - 1) \times B(h_l) \quad (7)$$

The variations in the grey level  $T_l$  may be calculated using the standard histogram equalization method:

$$\Delta T_l = (P - 1) \times Q (h_l) \quad (8)$$

Equation (7) states that the PDF of the input picture at grey level  $h_l$  is directly related to the space between  $T_l$  and  $T_l + 1$ . Equation (5)'s quantization operations and summarizing characteristics lead to negative implications of the standard histogram equalization approach (HE). It changes how the intensities of pixels are spread out in an image's histogram, making the distribution of intensities more even. Dark and bright areas become easier to tell apart, making it easier to see details and improving the general contrast of the picture. By making the sharpness range wider, HE helps bring out small details that might be hidden in areas that are underexposed or overexposed.

### **3.1.3 Image dividing using Contrast-Limited Adaptive Histogram Equalization (CLAHE)**

The modified component of AHE is contrast-constrained adaptive equalization. In this instance, the transformation function is produced by applying the expansion function to each nearby pixel. In contrast to AHE, it regulates variation. The CLAHE algorithm is provided as algorithm 1.

---

#### **Algorithm 1: CLAHE**

---

**Input:** “Low contrast color image”

**Output:** Enhanced picture with restricted adaptive histogram equalization contrast

**Stage 1:** A low- illumination image acquisition procedure

**Stage 2:** Get each input value utilized in the expansion process separately, including the number of rows and columns of segments, the dynamic range, the clip range, and the kind of distribution.

**Stage 3:** Sub-images of the actual are processed earlier.

**Stage 4:** The method is then used on the tile.

**Stage 5:** Invent a clipped histogram and a grayscale mapping. Because the numbers of environmental regions are spread uniformly across pixels at each gray stage, the mean amount of pixels in the gray condition may be defined as follows:

$$M_{avg} = \frac{M_{DQ-W_O} * M_{DQ-Z_O}}{M_{gray}} \quad (9)$$

$M_{gray}$  = No. of pixels in Y direction of “contextual region.”

$M_{DQ-W_O}$  = No. of gray level contextual

$M_{DQ-Z_O}$  = No. of pixels in X “direction of the contextual region.”

$M_{avg}$  = Median value of pixels

The actual clip limit,

$$M_{DK} = M_{CLIP} * M_{avg} \quad (10)$$

**Stage 6:** Enhance images by interrupting gray-level mapping. In this method, use the 4-pixel cluster and apply the “mapping process” to slightly overlay each mapping tile on the picture region, extract one pixel, and apply 4 mappings per pixel. Merge, improve, and repeat.

---

This method is used to improve contrast in localized regions. It divides an image into smaller blocks and applies histogram equalization independently to each block, preventing excessive amplification of noise. The contrast enhancement is limited using a predefined threshold, ensuring that extreme contrast modifications are controlled.

### **3.1.4 Image histogram using brightness preserving dynamic fuzzy histogram equalization (BPDFHE)**

This is an improved method to improve an image's contrast yet preserve the original image's brightness. It is especially helpful in situations where keeping the general brightness is essential, like low-light environments. Fuzzy equalization and histogram equalization are both used in BPDFHE. The first step is to break the image into several smaller sections, known as "patches." The pixel intensities are used to determine the fuzzy membership function for each block. Fuzzy logic allows for a gradual change in intensity, representing the fuzzy borders between visual sections.

The fuzzy membership function is used to dynamically equalize the histograms of each block. Instead of giving a uniform enhancement to the entire image, this adaptive method ensures that the enhancement is localized and varies depending on the features of the individual blocks. To further ensure that the overall brightness level is not significantly impacted throughout the enhancement process, BPDFHE includes a brightness preservation stage. To do this, the contrast of the original image was modified considering the intensity distribution of the environment. Brain MRI analysis enhances image details and highlights abnormalities, aiding medical professionals in diagnosis and treatment planning.

### **3.2 Segmentation using Fuzzy C-Means Adaptive Convolutional Long/Short-Term Memory (FCM-CLSTM)**

### 3.2.1 Fuzzy C-Means Clustering (FCM)

FCM Clustering is a common pattern recognition method. It extends K-Means. FCM lets data points belong to numerous clusters with fuzzy membership values between 0 and 1. FCM considers the likelihood of data points belonging to many clusters instead of one. It can handle ambiguous data due to its versatility. Image segmentation, data categorization, and clustering problems with unclear cluster boundaries employ it. Each data point may comprise a part of multiple groups at once when using fuzzy clustering.  $W$  represents the collection of  $M$  feature vectors, and  $d$  denotes the total number of groups. Minimizing the objective function  $I_n(V, U: W)$  is the central idea behind the FCM algorithm.

$$\min I_n(V, U: W) = \sum_{j=1}^d \sum_{i=1}^M \mu_{ji}^n \left\| w_j - u_j \right\|^2 \quad (11)$$

$$\text{subject to } \sum_{j=1}^d \mu_{ji} = 1, \quad 1 \leq i \leq M \quad (12)$$

Fuzzy partition matrix over set  $W$  into  $c$  equivalence classes, with cluster prototype  $U = \{u_j\} c \times n$ , and fuzzifier constant  $m \in (1, \inf)$ . The notation  $ij$  indicates that the  $i^{\text{th}}$  element belongs to the  $j^{\text{th}}$  cluster, while  $u_j$  denotes the location of the  $j^{\text{th}}$  cluster's nucleus. The Lagrange method of an unknown multiplier yields the following expressions for resolving (Equation (11)):

$$\mu_{ji} = \frac{\left( \left\| w_j - u_j \right\|^2 \right)^{\frac{-1}{(m-1)}}}{\sum_{i=1}^d \left( \left\| w_j - u_j \right\|^2 \right)^{\frac{-1}{(m-1)}}} \quad (13)$$

$$u_j = \frac{\sum_{i=1}^M \mu_{ji}^n w_j}{\sum_{j=1}^M \mu_{ji}^n}, \quad 1 \leq j \leq d \quad (14)$$

For Brain MRI segmentation, FCM is a highly effective technique. It provides membership degrees to picture pixels based on their intensity levels, which indicate how likely it is that they belong to a given cluster. Gray matter, white matter, and cerebrospinal fluid can all be distinguished with the aid of FCM in Brain MRI segmentation. Fuzzy methods account for pixels that belong to more than one cluster, and so capture the hazy nature of tissue borders. Because of its adaptability, FCM has proven to be an invaluable resource in the study of neuroimaging and the diagnosis and treatment of brain illnesses.

### 3.2.2 Convolutional Long/short term memory (CLSTM)

Combining the advantages of both CNNs and LSTM networks CLSTM is a hybrid neural network design with promising applications. It is designed toward handling spatial-temporal content like images or sequences of data. To enable the model to learn spatial characteristics while simultaneously capturing temporal dependencies, CLSTM integrates convolutional operations into the LSTM architecture. This allows it to discern spatial and temporal patterns and correlations with great accuracy.

$$j_s = \sigma(X_{wj} * W_s + X_{gj} * G_{s-1} + X_{dj} \circ D_{s-1} + a_j) \quad (15)$$

$$e_s = \sigma(X_{we} * W_s + X_{ge} * G_{s-1} + X_{de} \circ D_{s-1} + a_e) \quad (16)$$

$$\tilde{D}_s = \text{tang}(X_{wd} * W_s + X_{gd} * G_{s-1} + a_d) \quad (17)$$

$$D_s = e_s \circ D_{s-1} + j_s \circ \tilde{D}_s \quad (18)$$

$$p_s = \sigma(X_{wp} * W_s + X_{gp} * G_{s-1} + X_{dp} \circ D_s + a_p) \quad (19)$$

$$G_s = p_s \circ \text{tang}(D_s) \quad (20)$$

Where  $W$  is the input to the current cell,  $Ht1$  is the output, and  $Ct1$  is the state of the previous cell. The convolution kernels  $X_j$  (input gate),  $X_e$  (forget gate), and  $X_p$  (output gate) produce  $Ht$  (output gate). The Hadamard product, the nonlinear activation function, and the convolution operation are denoted as  $w, g, \text{and } \sigma.$ , respectively. There exist two distinct types of convolution kernels as described in equation (1). Specifically,  $X_w$  represents the weight of the input gate, which has dimensions of  $l \times l \times C \times S$ .  $X_p$  refers to a convolution filter of the output gate, with dimensions of  $l \times l \times S \times S$ . In this context,  $l$  represents the kernel size, while  $C$  and  $S$  denote the number of channels in the inputs and outputs, respectively.

In Brain MRI, CLSTM is often used to learn complex spatial and temporal patterns from image sequences, such as time series of brain scans or 3D volumes. In neuroimaging applications like brain tumor segmentation, lesion identification, and disease progression monitoring, this enables the model to more accurately capture spatial structures and temporal changes, producing more accurate findings.

The FCM Clustering technique is used to divide the dataset into fuzzy clusters as the first step in the FCM-CLSTM approach. This stage enhances later analysis by capturing ambiguity and overlaps in real-world data. The CLSTM network handles the data once it has been clustered.

Perfect for time series and image data, CLSTMs may concurrently learn spatial patterns and temporal correlations. The hybrid model leverages the feature learning and temporal dependency modeling capabilities of CLSTM in conjunction with FCM's capacity to incorporate uncertainty and flexibility. This FCM-CLSTM method provides more precise and reliable MRI segmentation. FCM provides an efficient clustering technique, and CLSTM helps with comprehending the geographical context. Together, these two components can process intricate MRI structures and enhance segmentation accuracy, which may contribute to greater precise diagnosis and treatment planning in neuroimaging.

#### 4. Result

We used Python 3.10 to implement our proposed methodology, and Windows 10's system setup contains Python 3.10, which is compatible with Pytorch 2.0. The system's powerful Ryzen 7 5800X CPU and effective Radeon RX 7900 XTX graphics card provide a strong basis for challenging machine learning tasks. The Brats 2021 dataset is taken from Brats 2021. There are 98 examples of healthy brains and 155 examples of abnormal brains included. Both sets of data include JPG files.

The original image and Normalized Median Filter (NMF) preprocessed image is displayed in Figure 2. The original image and equalized image are shown in Figure 3. HE frequency is presented in Figure 4. Input and output images produced using Contrast Limited “Adaptive Histogram Equalization (CLAHE)” are presented in Figure 5 and the frequency result of CLAHE is presented in Figure 6. Brightness Preserving Dynamic Fuzzy Histogram Equalized (BPDFHE) input and an output image and frequency were displayed in Figures 7 and 8, respectively. FCM segmentation input and output image is displayed in Figure 9.

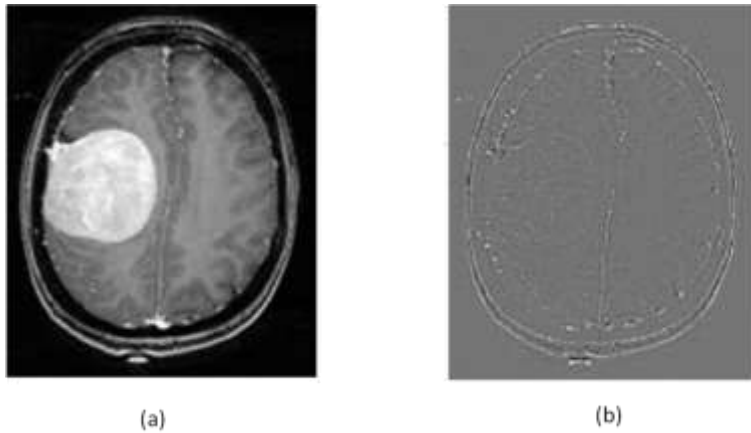


**Figure 2: Normalized Median Filter (a) original image (b) Preprocessed image**

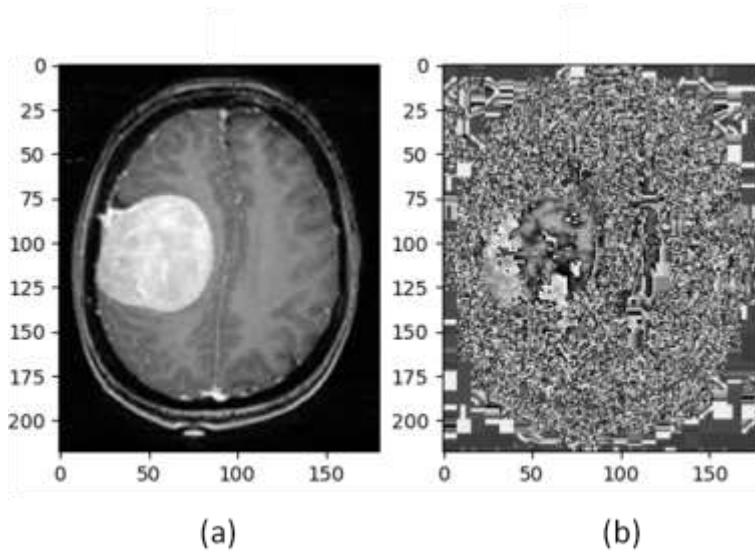


**Figure 3: HE (a) original image (b) equalized image**

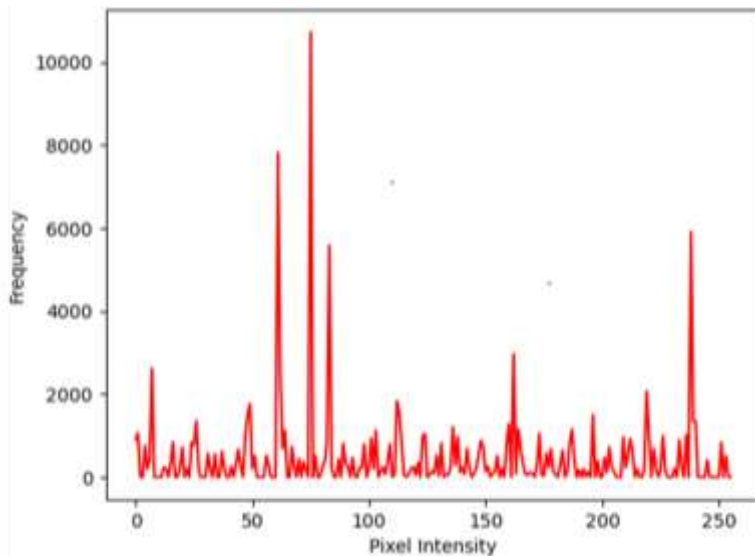


**Figure 4: Histogram Equalization (HE)**

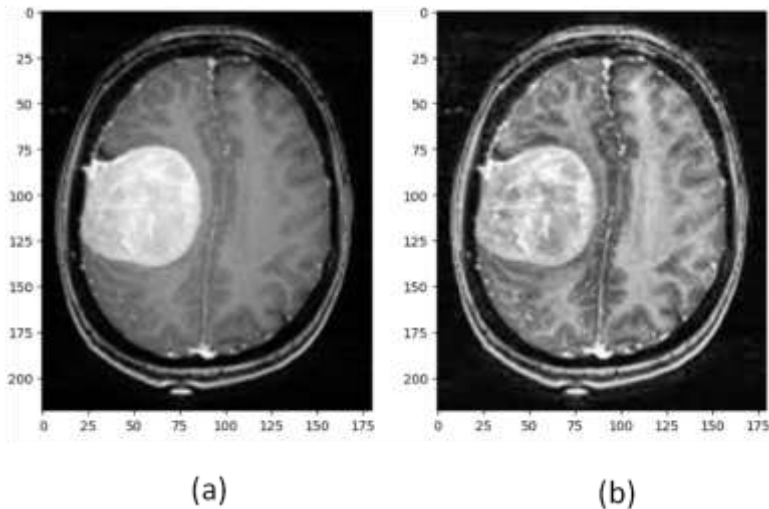


**Figure 5:** CLAHE (a) input image (b) output image

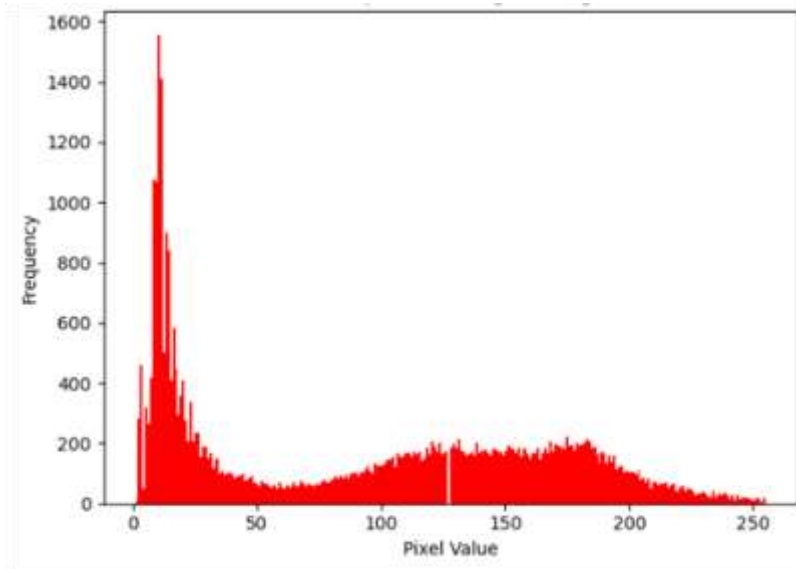


**Figure 6:** Contrast Limited Adaptive Histogram Equalization (CLAHE)

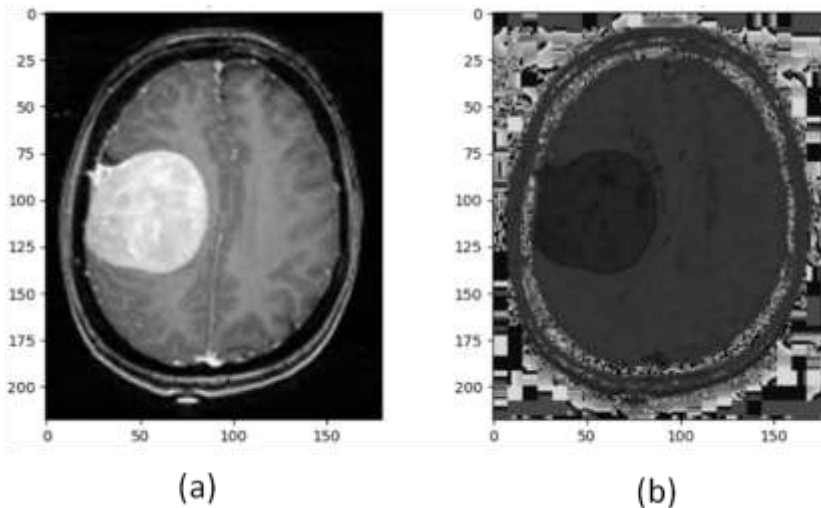


**Figure 7: BPDFHE (a) input image (b) output image**

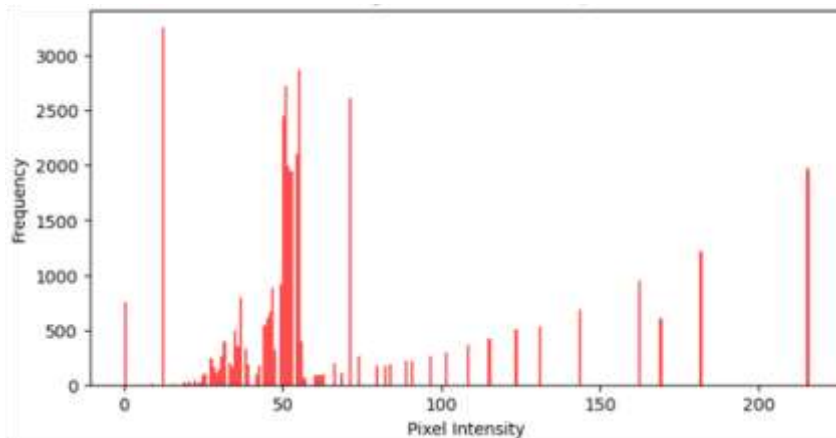
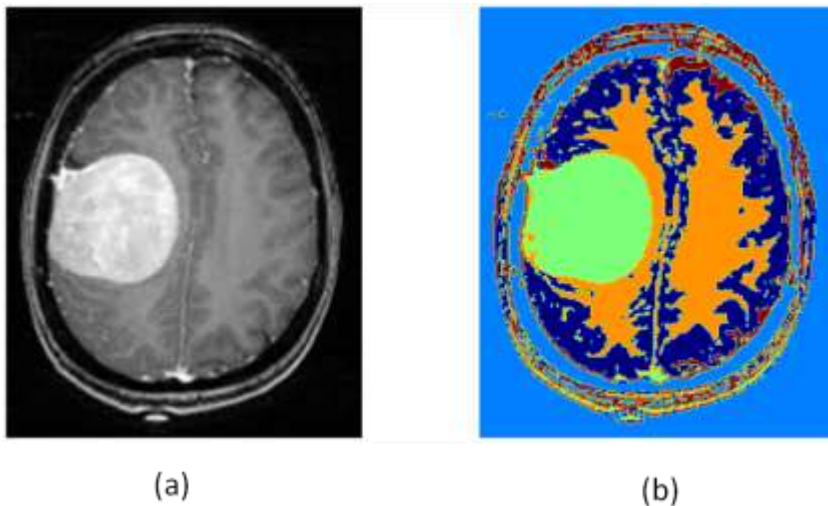


**Figure 8: Brightness Preserving Dynamic Fuzzy Histogram Equalization (BPDFHE)**



(a)

(b)

**Figure 9: FCM (a) input image (b) output image**

Accuracy measures pixel or voxel classification accuracy. Loss is a mathematical measure of the variance between the expected segmentation. The optimization aim during training guides the model to reduce the difference between expected and actual segmentations, enhancing segmentation accuracy. The accuracy and losses of our proposed methodology are presented in Table 1 and Figure 10.

**Table 1: Accuracy and loss**

Epochs	Values	
	Accuracy	Loss
10	1.8108	0.7426
20	1.619	0.7871
30	1.5757	0.7376
40	1.3921	0.7277
50	1.2679	0.802

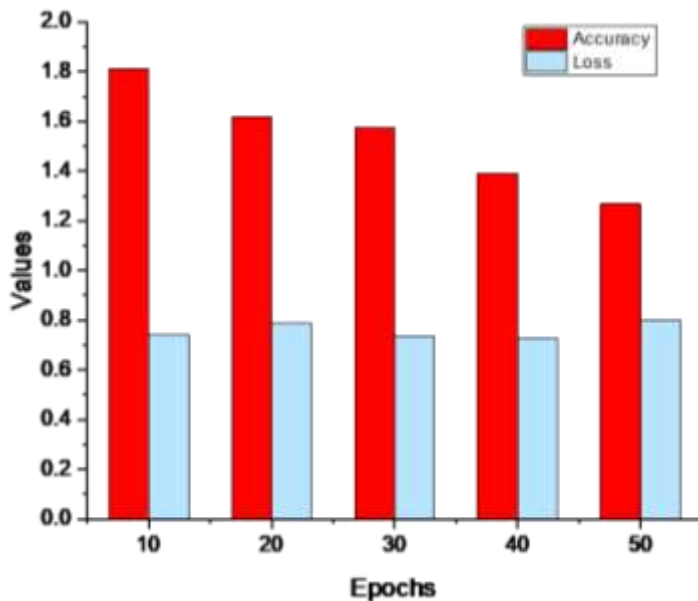


**Figure 10: Accuracy and loss**

The comparison analysis is done on “accuracy (%), precision (%), recall (%), F1-score (%), RMSE, AMBE, and MSE with the existing methodologies MCNN1, Yazdan et al. [16], CNN, Muiz, Fayyaz et al. [17], AlexNet, Yazdan et al. [16], MF-PDE, Priya Henry et al. [18], Adaptive Clip Limit Tile Size Histogram Equalization (ACLTSHE), Fawzi et al. [19], K-Nearest Neighbor (K-NN), Mittal et al. [20], and Self Organizing Map (SOM), Mittal et al. [20]” are compared with the proposed method FCM-CLSTM.

Accuracy measures the proportion of correctly classified pixels in the segmented image compared to the ground truth. It quantifies the model's ability to accurately identify different brain structures, providing an overall asset of segmentation performance. A high level of accuracy indicates efficient results. Table 2 and Figure 11 show the accuracy of the proposed and existing methods. While MCNN1, CNN, and AlexNet only achieve an accuracy of 82.71, 84.14, and 84.55%, respectively, the suggested technique, FCM-CLSTM, achieves an accuracy of 88.24 %. The proposed approach by FCM-CLSTM is more accurate than the established ones. The following equation expresses the accuracy value.

$$Accuracy = \frac{(True\ Positives + True\ Negatives)}{Total\ Number\ of\ Instances} \quad (21)$$

**Table 2: Accuracy (%)**

Methods	Accuracy (%)
MCNN1 [16]	82.71
CNN [17]	84.14
AlexNet [16]	84.55
FCM-CLSTM (Proposed)	88.24

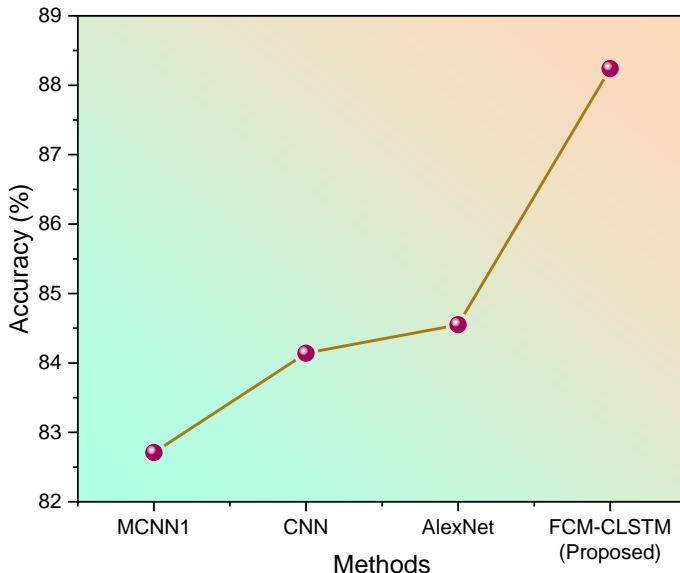


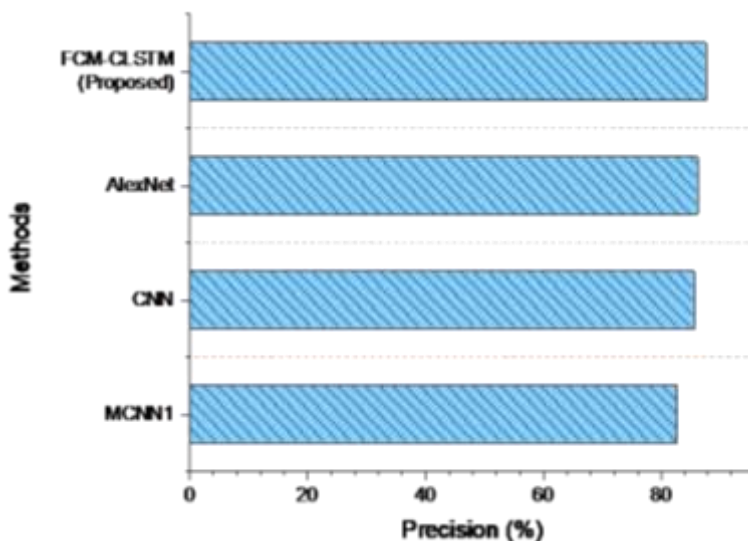
**Figure 11: Accuracy (%)**

Precision quantifies the accuracy of correctly identified positive (segmented) regions compared to all detected positive regions. It calculates the proportion of true positive pixels to the sum of true positive and false positive (misclassified) pixels, evaluating segmentation quality. A high level of precision suggests effective outcomes. Table 3 and Figure 12 show the accuracy value of the suggested and practiced processes. The suggested method, FCM-CLSTM, obtains a precision of 87.66%, while MCNN1, CNN, and AlexNet only accomplish 82.69, 85.63, and 86.20%, respectively. Compared to previous approaches, the FCM-CLSTM proposal has a high precision value. The equation to calculate the precision value is given below.

$$Precision = TP / (TP + FP) \quad (22)$$

**Table 3: Precision (%)**

Methods	Precision (%)
MCNN1 [16]	82.69
CNN [17]	85.63
AlexNet [16]	86.2
FCM-CLSTM (Proposed)	87.66

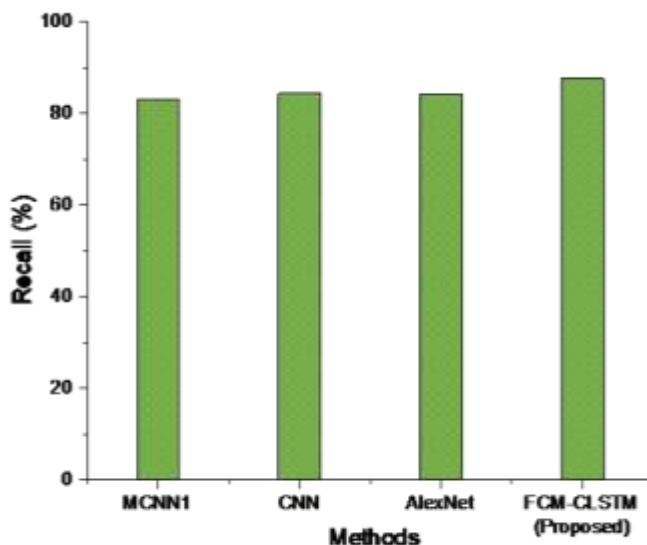
**Figure 12: Precision (%)**

Recall determines the proportion of true positive pixels over the overall number of real positive pixels in the ground truth. A high recall value indicates that the algorithm successfully captures most of the relevant brain regions in the segmentation, making it an important metric to assess the ability of the model to avoid missing significant structures in the MRI images. Table 4 and Figure 13 show the Recall value for the suggested and previously used methods. The suggested approach, FCM-CLSTM, obtains a Recall value of 87.66%, while MCNN1, CNN, and AlexNet only achieve 82.96%, 84.42%, and 84.26%, respectively. Comparing the FCM-CLSTM methodology to traditional methods, the Recall value is higher. The equation following is used to calculate the recall value.

$$Recall = TP / (TP + FN) \quad (23)$$

**Table 4: Recall (%)**

Methods	Recall (%)
MCNN1 [16]	82.96
CNN [17]	84.42
AlexNet [16]	84.26
FCM-CLSTM (Proposed)	87.66

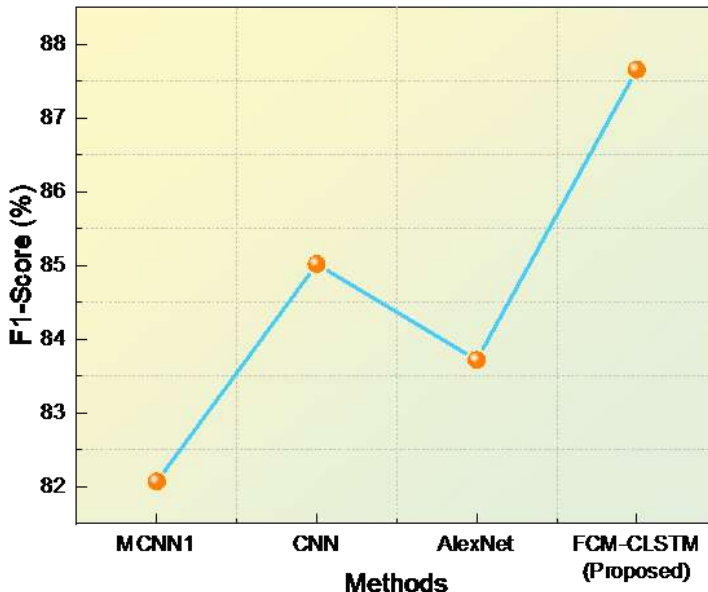
**Figure 13: Recall (%)**

The F1 score considers both precision and recall to provide a balanced measure of segmentation quality. The F1 score is calculated as the harmonic mean of “precision and recall”, ranging from 0 to 1”, with higher values indicating efficient segmentation accuracy in brain MRI images. Table 5 and Figure 14 show the F1 scores for the proposed and employed techniques. While MCNN1, CNN, and AlexNet only achieve an F1-score of 82.07 %, 85.02 %, and 83.72 %, respectively, the suggested technique, FCM-CLSTM, achieves an F-score of 87.66%. The FCM-CLSTM approach provides a greater F1 score as compared to other traditional approaches. The equation of the F1-score is mentioned below.

$$F1-score = 2 * (Precision * Recall) / (Precision + Recall) \quad (24)$$

**Table 5: F1-score (%)**

Methods	F1-Score (%)
MCNN1 [16]	82.07
CNN [17]	85.02
AlexNet [16]	83.72
FCM-CLSTM (Proposed)	87.66

**Figure 14: F1-score (%)**

The “Root Mean Squared Error (RMSE) measures the average difference between the predicted segmentation masks” and the ground truth labels, considering the squared differences to penalize larger errors more heavily. Lower RMSE values indicate better segmentation accuracy, indicating that the algorithm’s predicted masks closely align with the true segmentations in brain MRI images. Table 6 and Figure 15 show the RMSE of the proposed and employed methods. The suggested approach, FCM-CLSTM, achieves an RMSE

of 1.2132, but RMSEs of 4.959 and 0.3430 are only attained by MF-PDE, and ACLTSHE, respectively. Compared to conventional approaches, the FCM-CLSTM RMSE is lower. The equation for RMSE is as follows:

$$RMSE = \sqrt{\frac{1}{n} * \sum (predicted - actual)^2} \quad (25)$$

Average Mean Bias Error (AMBE) evaluates the average difference between the “predicted and ground truth segmentation masks”. It measures the overall accuracy of the model in capturing segmentation boundaries. A positive AMBE indicates an overestimation of the segmented regions, while a negative AMBE implies an underestimation. Ideally, AMBE should be close to zero for accurate and unbiased segmentation results. The lowest AMBE value as it indicates better accuracy and reliability in identifying brain structures. Table 6 shows the AMBE and RMSE of the proposed and employed methods. The suggested approach, FCM-CLSTM, achieves an AMBE of 0.000, but AMBEs of 0.017 and 4.179 are only attained by MF-PDE, and ACLTSHE, respectively. Compared to conventional approaches, the FCM-CLSTM AMBE is better. The equation for AMBE is as follows:

$$AMBE = (1 / N) * \sum (predicted - actual) \quad (26)$$

**Table 6: RMSE and AMBE**

Methods	RMSE	AMBE
MF -PDE [18]	1.2132	0.017
ACLTSHE [19]	4.959	4.174
FCM - CLSTM (Proposed)	0.343	0.000

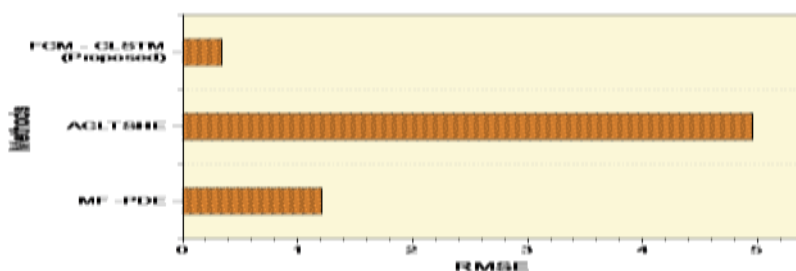


**Figure 15: RMSE**

Mean Squared Error (MSE) is a way to measure how different the expected segmentation masks are from the ground truth segmentation masks on average. A smaller error in segmentation and better matching of segmented areas with the actual brain structures are indications of better performance, which is shown by lower MSE values.  $m$  is the number of data points. *Actual value* represents the true target (ground truth) value for a data point. *The predicted value* represents the predicted value for the corresponding data point. Table 7 and Figure 16 show the MSE of the proposed and employed methods. The suggested approach, FCM-CLSTM, achieves an MSE of 0.1176, but MSEs of 0.2300, and 0.2560 are only attained by K-NN and SOM, respectively. Compared to conventional approaches, the FCM-CLSTM MSE is lower. The equation for MSE is as follows:

$$MSE = (1/m) * \Sigma(actual_{value} - predicted_{value})^2 \quad (27)$$

**Table 7: MSE**

Methods	MSE
K-NN [20]	0.23
SOM [20]	0.256
FCM-CLSTM (Proposed)	0.1176

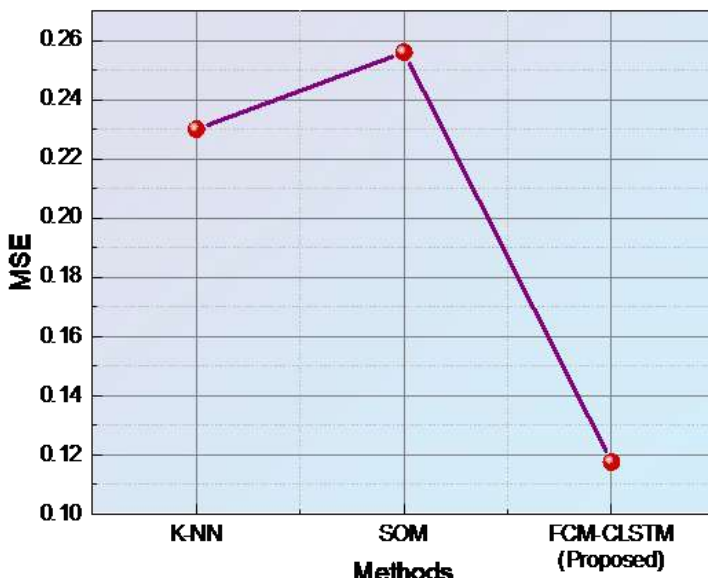


**Figure 16: MSE**

“PSNR (Peak Signal-to-Noise Ratio) measures the difference between the original segmented image and the reconstructed version in decibels (dB)”. Higher PSNR values indicate better segmentation accuracy and preservation of details. However, it's essential to consider other metrics, as PSNR may not fully reflect the perceptual quality and clinical relevance of the segmentation results. Our proposed method PSNR value is displayed in Table 8. The equation for PSNR is as follows:

$$PSNR = 10 * \log10 \left( \frac{MAX^2}{MSE} \right) \quad (28)$$

**Table 8: PSNR**

Method	PSNR
FCM-CLSTM (Proposed)	9.29 dB

**5. Conclusion**

Tumor identification and MRI picture segmentation is a relatively recent field of research. Several methods have been developed for this purpose. In this research, we presented a method for effective threshold and region-based segmentation using fuzzy c-means adaptive convolutional long/short-term memory (FCM-CLSTM). We gathered the Brats 2021 dataset for this study. The present study assessed the effectiveness of the methods currently in use using a number of metrics, including “accuracy (88.24%), precision (87.66%), recall (87.66%), F1-score (87.66%), RMSE (0.343), AMBE (0.0), and MSE (0.1176)”. The experimental outcomes of the suggested approach demonstrated superior performance compared to the existing method in the segmentation of brain MRI. Additional investigation is required to efficiently address possible obstacles and optimize the efficacy of the suggested methodology for the identification and segmentation of brain MRI. In the future, further enhancements can be explored to optimize brain MRI segmentation and tumor detection. Research should focus on integrating advanced deep learning techniques to improve accuracy and efficiency.

**References**

1. Ajagbe, S.A., Amuda, K.A., Oladipupo, M.A., Oluwaseyi, F.A. and Okesola, K.I., 2021. Multi-classification of Alzheimer's disease on magnetic resonance images (MRI) using deep convolutional neural network (DCNN) approaches. International Journal of Advanced Computer Research, 11(53), p.51.
2. Dash, S., Shakyawar, S.K., Sharma, M. and Kaushik, S., 2019. Big data in healthcare: management, analysis, and prospects. Journal of big data, 6(1), pp.1-25.

3. Wadhwa, A., Bhardwaj, A. and Verma, V.S., 2019. A review on brain tumor segmentation of MRI images. *Magnetic resonance imaging*, 61, pp.247-259.
4. Lillington, J., Brusaferri, L., Kläser, K., Shmueli, K., Neji, R., Hutton, B.F., Fraioli, F., Arridge, S., Cardoso, M.J., Ourselin, S. and Thielemans, K., 2020. PET/MRI attenuation estimation in the lung: a review of past, present, and potential techniques. *Medical physics*, 47(2), pp.790-811.
5. Niu, X., Zhang, F., Kounios, J. and Liang, H., 2020. Improved prediction of brain age using multimodal neuroimaging data. *Human brain mapping*, 41(6), pp.1626-1643.
6. Dalca, A.V., Yu, E., Golland, P., Fischl, B., Sabuncu, M.R. and Eugenio Iglesias, J., 2019. Unsupervised deep learning for Bayesian brain MRI segmentation. In *Medical Image Computing and Computer Assisted Intervention–MICCAI 2019: 22nd International Conference, Shenzhen, China, October 13–17, 2019, Proceedings, Part III 22* (pp. 356-365). Springer International Publishing.
7. Coupé, P., Mansencal, B., Clément, M., Giraud, R., de Senneville, B.D., Ta, V.T., Lepetit, V. and Manjon, J.V., 2020. *AssemblyNet*: A large ensemble of CNNs for 3D whole brain MRI segmentation. *NeuroImage*, 219, p.117026.
8. Palumbo, L., Bosco, P., Fantacci, M.E., Ferrari, E., Oliva, P., Spera, G. and Retico, A., 2019. Evaluation of the intra-and inter-method agreement of brain MRI segmentation software packages: A comparison between SPM12 and FreeSurfer v6. 0. *Physica Medica*, 64, pp.261-272.
9. Wu, W., Li, D., Du, J., Gao, X., Gu, W., Zhao, F., Feng, X., and Yan, H., 2020. An intelligent diagnosis method of brain MRI tumor segmentation using deep convolutional neural network and SVM algorithm. *Computational and Mathematical Methods in Medicine*, 2020.
10. Anand, L., Rane, K.P., Bewoor, L.A., Bangare, J.L., Surve, J., Raghunath, M.P., Sankaran, K.S. and Osei, B., 2022. Development of machine learning and medical-enabled multimodal for segmentation and classification of brain tumors using MRI images. *Computational Intelligence and Neuroscience*, 2022.
11. Vang, Y.S., Cao, Y., Chang, P.D., Chow, D.S., Brandt, A.U., Paul, F., Scheel, M. and Xie, X., 2020, April. *SynergyNet*: a fusion framework for multiple sclerosis brain MRI segmentation with local refinement. In *2020 IEEE 17th International Symposium on Biomedical Imaging (ISBI)* (pp. 131-135). IEEE.
12. Myint, H.H. and Aung, S.L., 2020. An efficient tumor segmentation of MRI brain images using thresholding and morphology operation (Doctoral dissertation, MERAL Portal).
13. Khairandish, M.O., Sharma, M., Jain, V., Chatterjee, J.M. and Jhanjhi, N.Z., 2022. A hybrid CNN-SVM threshold segmentation approach for tumor detection and classification of MRI brain images. *Irbm*, 43(4), pp.290-299.
14. Arshad, H.S., 2020. Brain Tissues Segmentation using Pre-Training based Pipeline and Customized Loss Functions (Doctoral dissertation, Pakistan Institute of Engineering & Applied Sciences).
15. Alhassan, A.M. and Zainon, W.M.N.W., 2020. BAT algorithm with fuzzy C-ordered means (BAFCOM) clustering segmentation and enhanced capsule networks (ECN) for brain cancer MRI image classification. *IEEE Access*, 8, pp.201741-201751.
16. Yazdan, S.A., Ahmad, R., Iqbal, N., Rizwan, A., Khan, A.N. and Kim, D.H., 2022. An efficient multi-scale convolutional neural network-based multi-class brain MRI classification for SaMD. *Tomography*, 8(4), pp.1905-1927.
17. Muiz Fayyaz, A., Kolivand, M., Alyami, J., Roy, S. and Rehman, A., 2022. Computer Vision-Based Prognostic Modelling of COVID-19 from Medical Imaging. In *Prognostic Models in Healthcare: AI and Statistical Approaches* (pp. 25-45). Singapore: Springer Nature Singapore.
18. Priya Henry, A.G. and Jude, A., 2021. Convolutional neural-network-based classification of retinal images with different combinations of filtering techniques. *Open Computer Science*, 11(1), pp.480-490.

19. Fawzi, A., Achuthan, A. and Belaton, B., 2021. Adaptive Clip Limit Tile Size Histogram Equalization for Non-Homogenized Intensity Images. *IEEE Access*, 9, pp.164466-164492.
20. Mittal, M., Goyal, L.M., Kaur, S., Kaur, I., Verma, A. and Hemanth, D.J., 2019. Deep learning-based enhanced tumor segmentation approach for MR brain images. *Applied Soft Computing*, 78, pp.346-354.

## Authors Profile



**AKM B. HOSSAIN** received a B.Sc. degree from the University of Pune, Bachelor of Computer Science (BCS), Pune, India, in 2000, and an M.Sc. degree in Masters of Communication Engineering (MSCE) from United International University (UIU), Dhaka, Bangladesh, in 2009. He is currently pursuing a PhD degree with the Faculty of Engineering in the School of Computing, Universiti Teknologi Malaysia (UTM), Malaysia, and previously worked with King Khalid University (KKU), the University of Bisha (recent), Saudi Arabia, Department of Information Systems and Cyber Security, under the Ministry of Education. His current research interests are data augmentation, deep learning, segmentation, and Artificial Intelligence.



**DR. MD. SAH BIN HJ. SALAM** received the bachelor of science degree from the University of Pittsburgh, Pittsburgh, PA, USA, and the master's and Ph.D. degrees in computer science with a specialization in speech processing and AI from the University of Technology Malaysia. His research work is mainly in speech processing, computer vision, and machine learning. He is currently serving as a Senior Lecturer and researcher at VicubeLab, the Faculty of Computing, Universiti Teknologi Malaysia.



**MUHAMMAD SHAMSUL ALAM** received a B.Sc. degree from the Jahangirnagar University of Computer Science and Engineering, Dhaka, Bangladesh, in 2003 and an M.Sc. engineering in ICT from the Bangladesh University of Engineering and Technology (BUET), Dhaka, Bangladesh, in 2007. He is pursuing a Ph.D. at the School of Computing, Universiti Teknologi Malaysia (UTM), Malaysia. He previously worked with King Khalid University (KKU) and the University of Bisha (UB) under the Ministry of Education, Saudi Arabia. His current research interests are computer vision, machine learning, and software engineering.



### **DR. AHMAD FAHDIL YUSOF**

Is Senior Lecturer in the Faculty of Computing since 2015 and currently serves as the Mobility Manager in UTM International Office in Universiti Teknologi Malaysia (UTM). In this role, he has been responsible for managing, creating opportunities, and taking care the wellbeing of the mobility students in UTM. He holds a Ph.D. degree in Information Systems and graduated in 2015 with Best Students Award in UTM 54th Convocation Ceremony. His research interests include Information Systems Adoption, M-Health, and Education Informatics. He has published and co-authored numerous technical papers mainly in Information Systems area, has been the editors for several journals, book chapters and conference proceedings, besides serving as reviewers and technical committee members mainly in IEEE conferences including Scopus and ISI indexed proceedings and journals in related fields. He also had won several best paper awards in his publications. He had been involved with many research grants which mostly related to the Information Systems research area. Up until his 8 years of service in UTM, he had led around 3 research projects which had total cost around USD 148,540. In his service, he received the outstanding service award 2019 in Citra Karisma 2020 at university level and several times for department level in UTM.

**AKM BELLAL HOSSAIN** Works Flora Systems Ltd, As a Faculty Member of Different IT Courses like programming, Database, and Web design, Works as a Trainer of an IT Scholarship project ( IDB-BISEW ), Worked at Different National and International Universities As A Faculty member Teaching Different Subjects like Computer Programming C++, Java, Database Management System, MS-Access, MySQL, SQL Server, Oracle, Computer Network, Combinatorial Analysis of Computer, Computational Geometry, Computer Modeling & Simulation, Knowledge Base System-Commerce, Algorithms & Data Structures, Multimedia, Virtual Reality, Data Warehousing And Data Mining, Computer Games, Operating System, Principles of Information Systems, Decision Support Systems, Selected Topics, Industrial Training Supervision, Graduation Projects etc.